RTI Surface Normal Calibration with a 3D Printed Spatial Target: Turning Images into Data

Gregory Bearman[1], Eric Doehne[2], Dale Kronkright[3] and Marcello Manfredi[4]

[1]ANE Image, Pasadena CA. greg@aneimage.com; http://www.aneimage.com

[2]Conservation Sciences, Pasadena, CA. conservationsciences.org

[3]Georgia O'Keeffe Museum, Santa Fe NM.

[4]ISALIT-University of Piemonte Orientale, Alessandria, Italy; http://www.isalit.net

June 2, 2014

In the last decade, imaging has become an increasingly significant player in the analysis, preservation and dissemination of cultural heritage, especially in archeology, art, and conservation programs. As new imaging methods have been developed, they have routinely been applied to cultural heritage. Reflectance transformation imaging (RTI) has been widely used for the documentation of important heritage objects (Earl, Martinez, & Malzbender, 2010). The RTI method creates dynamic digital illumination models of the objects that let the user control the illumination angles in software. In essence, RTI captures how complex surfaces interact with light – a significant advance over single, static images. The original use was to look at objects in relief for interpretation and content, such a cuneiform tablets, rock glyphs and other objects where shadows and 3D are significant. It has expanded to texts and documentation as well. Our interest is in developing RTI as a new tool for detecting changes in cultural heritage objects over time to help conservators and others monitor and minimize such changes.

There is a pioneering program in place that uses spectral imaging to monitor changes in the Dead Sea Scrolls (Marengo et al., 2011). That project showed that quantitation and calibration are critical to creating an effective monitoring program. The method uses multi-variate statistics to analyze spectral reflectance data over the visible and near infra-red and provides an automatic way to interrogate large image data sets, something simply not possible to do by the human eye and inspection. Repeatable and reproducible measurement of the relevant parameter is key to tracking changes. In particular, the noise and uncertainty has to be well characterized. For example, in the case of reflectance measured between [0,1], a system with a standard deviation of ±0.5 is not useful.

By analogy with the Dead Sea Scroll work, RTI can monitor changes in the surface topography and overall shape of objects as they respond to changes caused by damage or deterioration (Manfreddi et al., 2013). While "universal" image changes such as object orientation, tip, tilt and rotation and "global" changes such as sensor and image file pixel density, focal length and optical aberrations require registration and correction steps in both the capture and processing workflows, detecting "local changes" in the surface morphology of an object as a result of damage or deterioration over time appear to be a practical goal of RTI. Imaging offers the possibility of alerting conservators and preservation managers to changes that are too small for the human observer to detect but

larger than the inherent variability of the capture process and the normal variability of the object in response to changing environmental conditions.

Canvas, wood, parchment and many other substrates change shape or expand and contract in response to humidity and temperature (Mecklenburg, 2007). RTI surface normals, which track the local orientation of a pixel, will move as an object changes shape.

Returning to our calibration theme, we created a 3D spatial target with fixed normals as a calibration tool. Theoretically, if we have a wedge of known surface angles in the field of view, the normals calculated from the surfaces of the wedge shape should all cluster around the known value, within the precision variability of the capture and processing workflows; the spread in the normals is a measure of how well we can use them to track local surface changes. The target does not create normals with absolute values we measure, but rather normals whose difference is fixed and known. If, for example, the spread of the normals values from a calibration target are less than 3%, then detected changes in the surface morphology of an object greater than 3% may alert a conservator that the object has suffered deterioration in a specific area. The absolute values of the normal reflection vectors depend on the tip and tilt of the base of the target, so there is really no way to measure it except relative to each other. Still, if we can establish that the accuracy of the calculated normals from an RTI image is within an acceptable range and the precision of the capture and processing workflows are known to be within acceptable range, change data and visualizations become meaningful values for detecting and monitoring the rate of deterioration of cultural heritage materials.

The target was made with 3D printing and consists of objects with surfaces whose normals we can easily calculate; planes, wedges and a cone. Shown in Figure 1, the target is 32 x 20 mm and the tallest object is 16 mm tall. It was made with a much higher z-step resolution (0.025 mm) than typical "home" 3D printers, which are typically ~ 0.1 mm or more in step and actually produce a pretty coarse object, requiring surface treatment. The plastic is quite dense and a laser showed that light does not penetrate, so there are minimal internal reflections and scattering to make surface location fuzzy as can happen with marble (Angelo, Levoy, & Blais, 2001).

We took two sets of RTI data, one moving the wireless flash by hand and the other with an automated articulated arm that moved the flash to fixed locations. Dale Kronkright at the Georgia O'Keeffe museum took the handset data and Dr. Marcello Manfredi acquired the data with a mechanic arm.

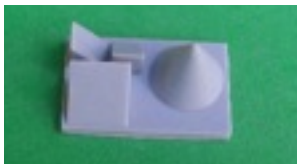

Figure 1. 3D printed spatial calibration target. Fabricated with 0.025 mm resolution, the target is quite smooth. It is opaque so there is minimal internal photon scattering to create confusion on the normal calculation. The target is 32 mm long.

For a perfect RTI system, we expect all normals to a plane to be the same; for our target that would mean on the wedge surfaces as well as a plane parallel to the cone axis and perpendicular to the base. Figure 2 shows a first cut analysis of the O'Keeffe data as a heat map showing the x values of the normals projected onto a plane. If the normals are all the same, then the color should be the same. There is a set of back-to-back wedges and also one oriented at 90^o to the pair. The idea behind having wedges at 90^o is to see if the errors in (x,y,z) depend on the surface orientation. In the case of a data set acquired by hand, not a dome, one can image undersampling in some locations that creates more errors in the normals in one direction. The two opposing wedges are basically the same color; the perpendicular wedge shows the effects of shadowing from the next-door wedge at the bottom of the wedge as it dies into the base plate. Clearly, that wedge should be rotated 180 and will we will do that in the next version.

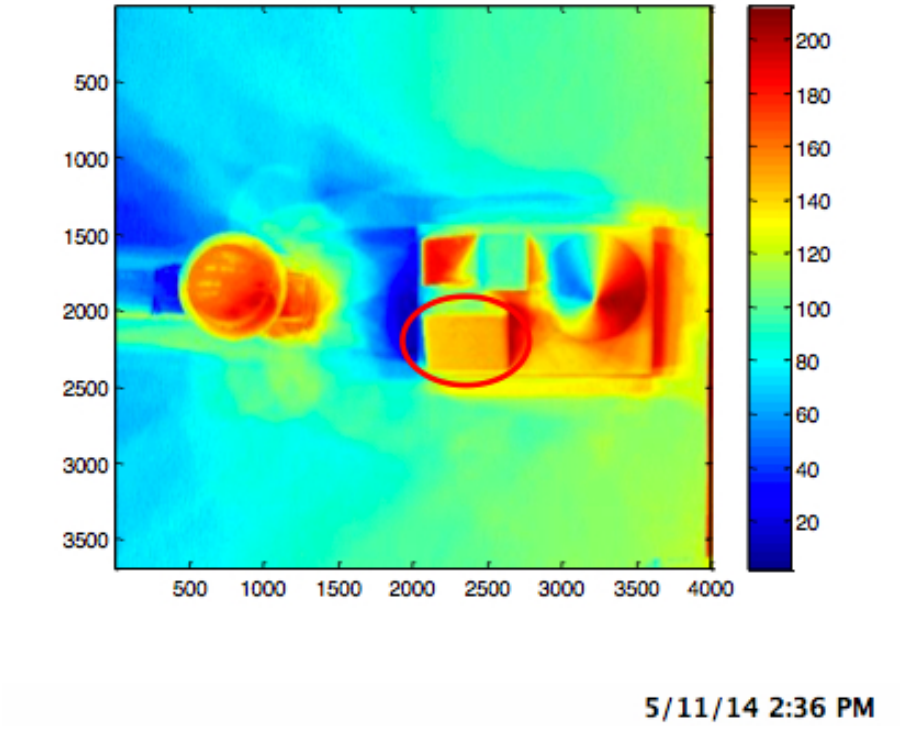

Figure 1. Heat map of the x value of the normals of the circled ROI on the calibration target. Note that each wedge surfaces appear to be about the same-see text for detailed numerical results. The sphere on the left is the reflective ceramic bearing used to detect the location of the flash highlights as part of the RTI captures process. Normals for the wedge surface should all be the same, the detailed statistics illustrate how well RTI can recover surface features.

Figures 2 and 3 show the same results for y and z components as well.

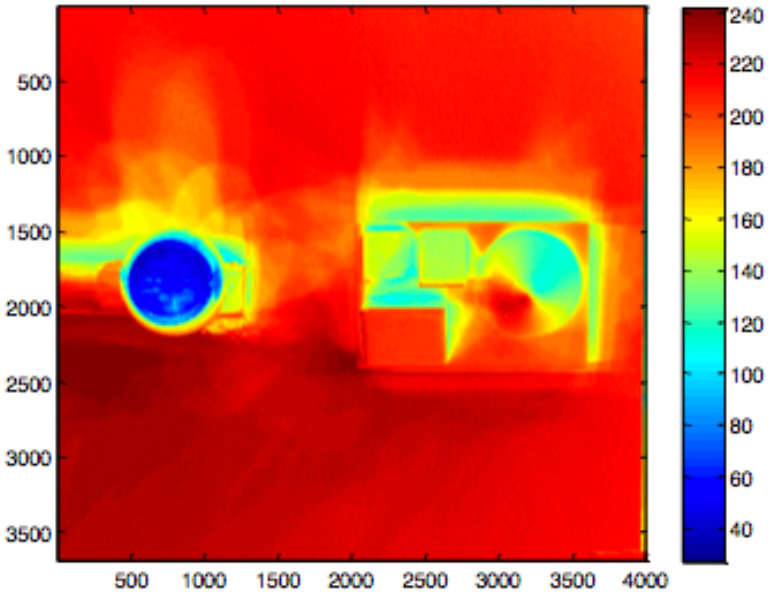

Figure 2. Heat map of the y component of the same ROI as in Figure 1.The units are pixels and note that the two back to back wedges are uniform in color, indicating we have retrieved the same normals.

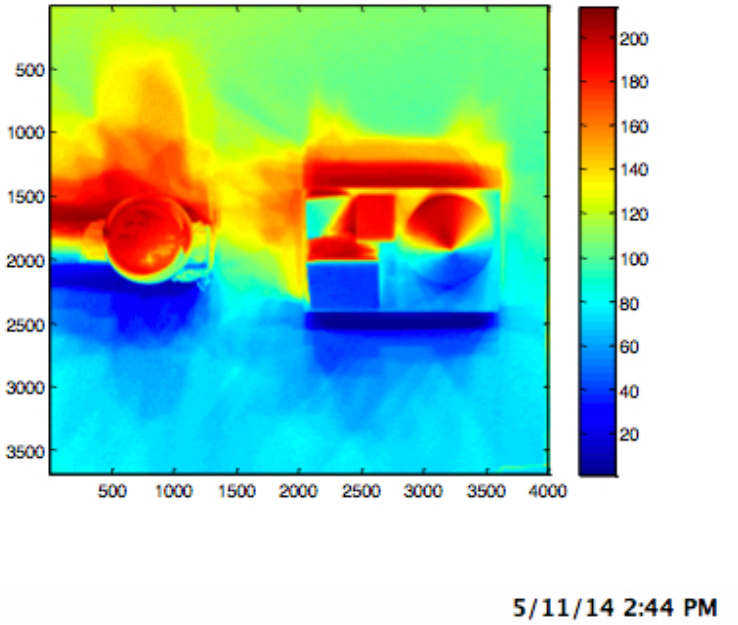

Figure 3. Heat map of the z component of the same target ROI as in Figure 1.The units are pixels.

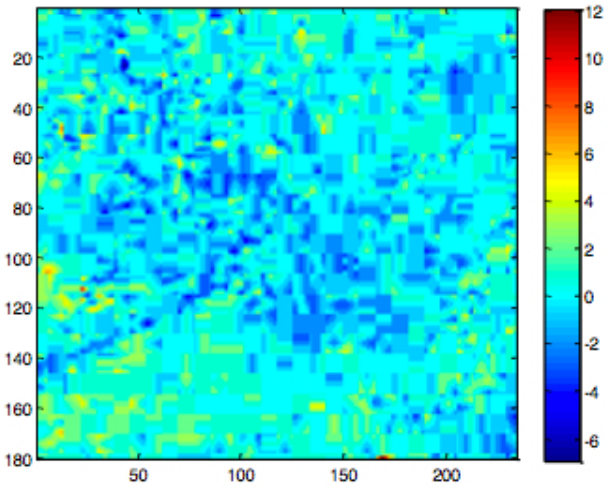

Figure 4. The difference from the mean for each pixel for the y component of the same area in Figure 2. This is an easy way to visualize the normal errors across the wedge. For this component, σ=1.3 pixels.

For the data shown, Table 1 presents the values and their distribution; the units are in pixels. If we translate pixels into linear scale on the target, it is ~20 μ/pixel, so our claim is that the RTI method is sensitive to changes ~30-40 microns of tip, tilt or piston of the surface, which is the normal σ scaled onto the target. This seems sensitive enough to detect shape changes caused by environmental effects such as humidity and temperature in many objects. For example, shape changes in the (x,y) plane of antiquarian parchment fragments over a few decades has been measured to be ~40-500 μ (Bearman, private communication). The height of paint features on a van Gogh was measured to be ~ 400 μ (Karaszewski et al., 2013), so our results should easily measure changes in surface topography on that scale. The Georgia O'Keeffe museum has seen lead soap micro bubbles on some paintings on the scale of 30-200 μ (Dale Kronkright, private communication); we have shown that RTI is sensitive to such changes even at the low end of the size range. The O'Keeffe Museum has a robust and active RTI program and has been adding the spatial target to all of its imaging sessions.

X component	146.8 ±1.9
Y component	38.9 ±1.3
Z component	203.9 ±1.3

Table 1. Normal components in Cartesian Coordinates for the wedge circled in Figure 1. Units are in pixels and the data is unbinned.

Note that the standard deviation is ~1-2 pixels, which is about the granularity of the imaging, suggesting it is about as good as it can get. Since we are not measuring better than 1 pixel, uncertainties of 1 pixel are basically measurement-limited and may not represent the ultimate ability of the method. As we are imaging at ~1200 dpi, this work suggests that the imaging scale is reflected in the RTI data quality and errors. If the errors are roughly constant in pixels, then imaging at half the resolution (twice the IFOV) halves the sensitivity of the method. We binned this data by two, halving the resolution and doubling the pixel size on the object; the standard deviations of the data were again ~1-2 pixels.

The next challenge becomes one of separating the detection of changes in morphology that could occur with normal and acceptable variations in object temperature, moisture content and orientation from changes that occur as a result of a deterioration process. For example, a slack, linen canvas support in an oil painting may undergo slight changes in planar deformation either as a result of changes in room temperature or humidity levels or simply as a result of the relative orientation of the painting relative to a vertical or horizontal position at the time of image capture. Separating data relevant to a dent, a sag in the canvas or the development of lead soap micro-protrusions within brush work from changes in normal reflection data which result from a tolerable change in moisture content will require more work on image registration, algorithms to define change and visualization of the results.

The target lets us compare absolute differences between known normals. We analyzed the normals in a plane through the wedges and perpendicular to base. In a perfect world, all the normals would be in the same plane and would have a difference in θ of 90 degrees, since the wedges are both 45^o. Since they are in the same plane, the difference in φ should be 180. The measured value for the θ difference is 93.72 and the 183.67 for φ. We ran a transect down one of the wedges, as shown in Figure 5; the standard deviation for θ and φ respectively are 0.89^o and 0.62^o. There is some anomaly at the top of the wedge in θ, cause unknown. One suggestion is that since the tip is thin, we are seeing the results of photon scattering; the counter augment is that there is no corresponding effect on the φ values. At the moment, we are assuming that the target itself has been produced correctly-the (x,y) accuracy of the machine is 27 μ and the z step was 25 μ. Note that this is about the IFOV for the scale of the imaging we did, but the binned data would have a pixel twice as big and 4 times the area.

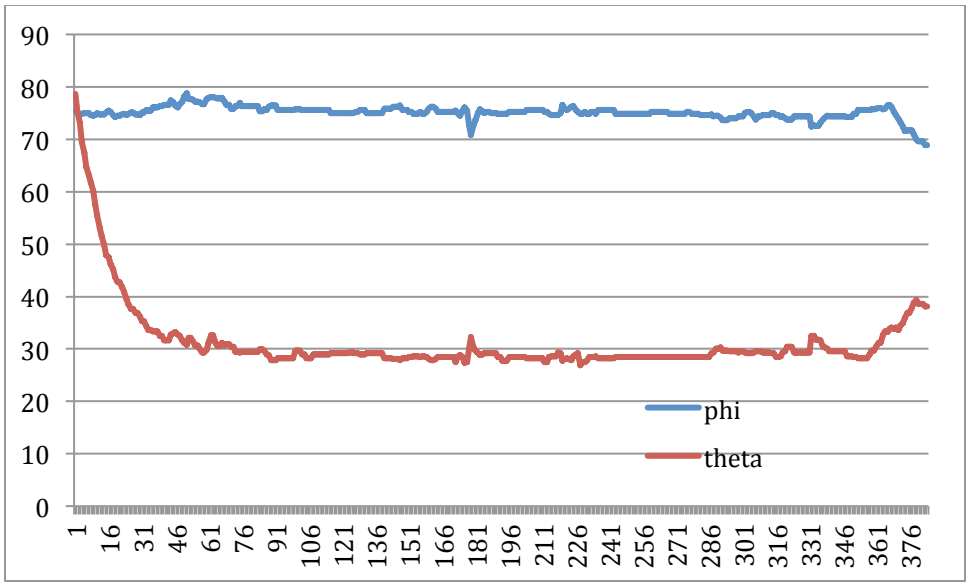

Figure 5. Spherical coordinates of normals in the same plane through the opposite wedge faces. The x-axis is pixels down the wedge with a corresponding linear scale of [0,7.5 mm].

The arm and the hand acquired set provided about the same spread in the normals. We are redesigning the target in light of the work here (for example, no shadowing) and will have more data and results to report on an upcoming journal article.

A recent paper presented a method to derive a 3D mesh or point cloud map of an object (Elfarargy, Rizq, & Rahswan, 2013) from an RTI file. While the accuracy of that still needs to be examined, it opens up complementary ways of thinking about detecting and visualizing change. For example, (Grosman, Karasik, & Harush, 2014) used 3D scanning to determine how stone tools' shape can be affected by river and shores. They tumbled modern knapped tools in a drum with pebbles and repeatedly imaged them. Using shape and asymmetry analysis (see (Saragusti, Karasik, Sharon, & Smilansky, 2005) they determined areas of material erosion and how the various facets and edges fared. Thinking of a 3D mesh leads one to imagine detecting change via a variety of image segmentation and feature analysis methods to fuse with the corresponding RTI view of the object.

BIBLIOGRAPHY

Angelo, G. G. M. R. J., Levoy, B. M., & Blais, L. C. F. (2001). An assessment of laser range measurement on marble surfaces. Presented at the 5th Conference onf optical 3D, Vienna.

Earl, G., Martinez, K., & Malzbender, T. (2010). Archaeological applications of polynomial texture mapping: analysis, conservation and representation. *Journal of Archaeological Science*, *37*(8), 2040–2050. doi:10.1016/j.jas.2010.03.009

Elfarargy, M., Rizq, A., & Rahswan, M. (2013). 3D Surface Reconstruction Using Polynomial Texture Mapping. *Advances in Visual Computing. Lectures Notes in*

Computer Science, *8033*, 353–362.
Grosman, L., Karasik, A., & Harush, O. (2014). Archaeology in Three Dimensions: Computer-Based Methods in Archaeological Research. *Journal of Eastern Mediterranean Archaeology and Heritage Studies*. doi:10.1353/ema.2014.0000
Karaszewski, M., Adamczyk, M., Sitnik, R., Michoński, J., Załuski, W., Bunsch, E., & Bolewicki, P. (2013). Automated full-3D digitization system for documentation of paintings, 87900X–87900X–11.
Manfreddi, M., Kronkright, D., Doehne, E., Jacobs, M., Marengo, E., & Bearman, G. (2013). Measuring Changes in Cultural Heritage Objects with Reflectance Transform Imaging. Presented at the Digital Cultural Heritage, Marseille.
Marengo, E., Manfredi, M., Zerbinati, O., Robotti, E., Mazzucco, E., Gosetti, F., et al. (2011). Technique Based on LED Multispectral Imaging and Multivariate Analysis for Monitoring the Conservation State of the Dead Sea Scrolls. *Analytical Chemistry*, *83*(17), 6609–6618. doi:10.1021/ac201068s
Mecklenburg, M. F. (2007). Micro climates and moisture induced damage to paintings. *Museum Microclimates Conference*.
Saragusti, I., Karasik, A., Sharon, I., & Smilansky, U. (2005). Quantitative analysis of shape attributes based on contours and section profiles in artifact analysis. *Journal of Archaeological Science*, *32*(6), 841–853. doi:10.1016/j.jas.2005.01.002